SIMULATION OF FUZZY BASED SOFT SWITCHED SINGLE SWITCH ISOLATED DC-DC CONVERTER

[1]PUSUKURU BAJI, [2]K.RAJESH,
[1]PG Student,Dept of EEE,Vignan's Lara Institute of Technology & sciences,Guntur,AP
[2] Assistant professor ,,Dept of EEE,Vignan's Lara Institute of Technology & sciences,Guntur,AP

Abstract*—This paper proposes a soft switching techniques by using the isolated DC-DC converter in a single switch. The proposed topology, based on the soft switching technique, uses only one switch to step up the mains voltage with high gain The proposed converter has able to offer reduced cost and high power density in boost application due to the following features: zero-current switching (ZCS) turn-on and zero-voltage switching (ZVS) turn-off of switch and ZCS turn-off of diodes regardless of voltage and load variation; low rated lossless snubber; reduced transformer volume compared to flyback-based converters due to low magnetizing current. By using the simulation results we can analyze the proposed method

***Index Terms*— Isolated step-up dc–dc converter, single switch, soft switching Component,**

I. INTRODUCTION

There has been an increasing interest in the soft-switching power conversion technologies in order to overcome the limitations of the hard-switching technologies [1]-[7]. Soft- switching (SS) converters had many advantages over hard- switching (HS) converters[2]. To reduce the cost of switches and the switching losses, only one switch is provided to the resonant converter. For output voltage stabilization a closed loop circuit with PI control is provided. So, when the load changes the output voltage is kept constant.

A closed loop control has high reliability, easy implementation and output short circuit and overload protection. The current-fed isolated converter has two types: passive clamped [5]–[7] and active-clamped [8]. The passive clamped current-fed converter has simple structure and small switch count, but suffers from excessive power losses dissipated in the RCD snubber and associated with hard switching of main switch. They achieve not only lossless clamping of voltage spikes caused by transformer leakage inductance but also zero-voltage switching (ZVS) turn on of switches. However, they may not be expected to achieve high efficiency and low cost in relatively low power application since they need at least four switches and gate driver circuits. Isolated converters with reduced switch count have been proposed for low power application [14]. Isolated dc–dc converters with one main switch and one clamp switch achieve converter. ZVS turn on of switches, but switches are turned off with hard switching [9]. Isolated single switch dc–dc converters are more attractive to achieve low cost [7].

ZCS–ZVS Z-source converter and flyback converter are hard switched at both turn-on and turn-off instants. An isolated single-switch resonant converter [6] achieves both ZCS turn-on and ZCS turn-off of switch, but need high transformer turn ratio for step-up application due to low voltage gain and hence is not suited to step-up application.

In this paper, a soft-switched single switch isolated converter is proposed for step-up application. The proposed converter has the following features: 1) ZCS turn-on and ZVS turn-off of switch regardless of voltage and load variation; 2) ZCS turn-off of all diodes leading to negligible voltage surge associated with the diode reverse recovery; 3) small input current ripple due to CCM operation; 4) reduced transformer volume due to low magnetizing current; and 5) low-rated lossless snubber, which makes it possible to achieve high efficiency and low cost for step-up application

II. PROPOSEDCONVERTER

Fig. 1 shows the circuit diagram of the proposed converter. The proposed converter consists of input filter inductorLi , switchS1, a lossless snubber which includes capacitor Cs,inductorLs, and diodes Ds1 andDs2, and clamp capacitor Cc at the primary side and Lr–Cr series resonant circuit and diodes D1andD2at the secondary side.

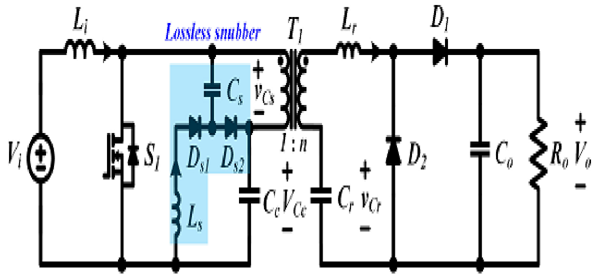

Fig. 1. Proposed isolated single switch

The lossless snubber makes it possible to achieve ZVS turn-off of switch as well as clamp the voltage spikes of the switch by leakage inductance. Also, the Lr–Cr series resonant circuit makes it possible to achieve ZCS turn-off of diodes. Fig. 2 shows three resonance operations according to the variations of resonant frequencyfr1 which is expressed as in (1): the above-resonance operation (DTs <0.5Tr1), the resonance operation (DTs =0.5Tr1), and the below-resonance operation (DTs >0.5Tr1)

$$f_{r1} = \frac{1}{T_{r1}} = \frac{1}{2\pi\sqrt{L_r C_r}} \quad (1)$$

It can be seen from Fig. 2 that the total switching losses are smaller for the below-resonance operation since both switch turn-off current and diode di/dt of the below-resonance operation are smaller than them of the above-resonance operation. Therefore, the below-resonance operation is chosen for the proposed converter.

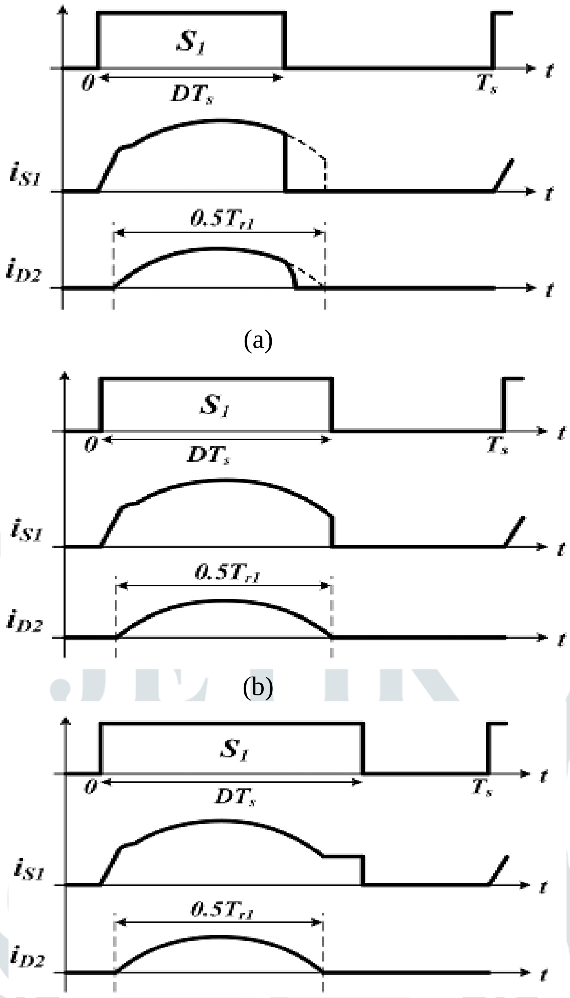

Fig. 2. Comparison of switch and diode current waveform according to variation offr1: (a) above-resonance operation (DTs <0.5Tr1), (b) resonance operation(DTs =0.5Tr1), and (c) below-resonance operation (DTs >0.5Tr1).

A. Operating Principles

Figs. 3 show key waveforms and operation states of the proposed converter in the below-resonance operation, respectively. In order to simplify the analysis of the steady-state operation, it is assumed that the input filter and magnetizing inductances are large enough so that they can be treated as constant current sources during a switching period. It is also assumed that clamp and output capacitances are large enough so that they can be treated as constant voltage sources during a switching period.

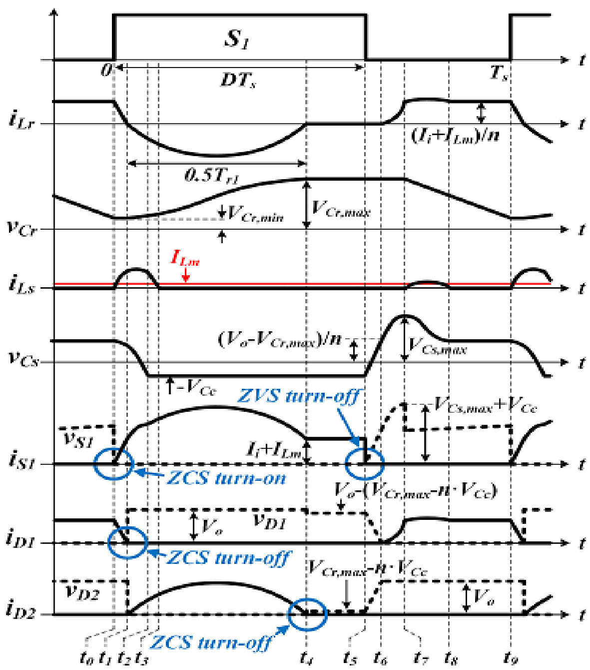

Fig. 3. Key waveforms of the proposed converter in the below-resonance operation

The voltage VCc across the clamp capacitor is the same as the input voltage Vi. In the below-resonance operation, nine modes exist within Ts. **Mode 1 (t0–t1):** This mode begins when switchS1 is turned ON. Equivalent circuit of this mode is shown in Fig. 4(a).Lsand Cs start resonating and resonant current iLs flows through Ls, Ds1, Cs, and S1. The voltage and current of resonant components are determined, respectively, as follows:

$$i_{Ls}(t) = v_{Cs}(t_o)\sqrt{\frac{C_s}{L_s}}\sin(\omega_{r2}(t-t_0)), t_0 < t < t_2 \quad (2)$$

$$v_{Cs}(t) = v_{Cs}(t_o)\ \cos(\omega_{r2}(t-t_0)), t_0 < t < t_2 \quad (3)$$

whereωr2 =1/ √ LsCs. Since induced voltage VCr, min–nVCc– Vo acrossLr makes time interval fromt0 to t1 very short, current iLr appears to decrease almost linearly. Current through S1 increases with the slope ofiLr, resulting in ZCS turn-on of S1. The turn-on loss of switch associated with energy stored in MOSFET's output capacitance is negligible in this low input voltage application. This mode ends when current iLr reaches 0 A. It is noted that diodeD1 is turned OFF under ZCS condition.

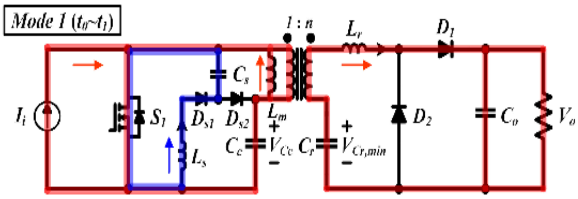

Mode 2 (t1–t2): This mode begins when current iLr changes its direction. Equivalent circuit of this mode is shown in Fig. 4(b).

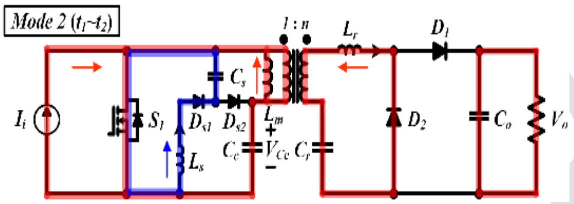

Lr andCr start resonating and resonant current iLr flows through Lr,Cr, andD2. The voltage and current of resonant components are determined, respectively, as follows.

$$i_{Lr}(t) = (V_{Cr,min} - nV_{Cc})\sqrt{\frac{C_r}{L_r}}\sin(\omega_{r1}(t-t_1))$$
$$t_1 < t < t_4 \quad (4)$$

$$v_{Cr}(t) = nV_{Cc} - (nV_{Cc} - V_{Cr,min})\cos(\omega_{r1}(t-t_1))$$
$$t_1 < t < t_4 \quad (5)$$

whereωr1 =1/ √ LrCr. When voltage across snubber capacitor Cs equals –VCc,Ls–Cs resonance ends.

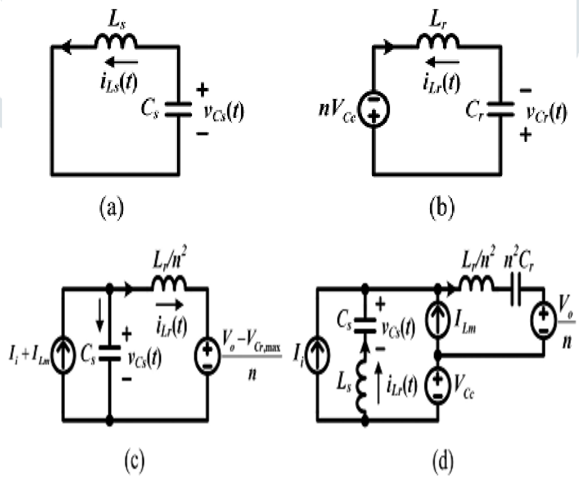

Fig. 4. Equivalent resonant circuits. (a) Mode 1–2 (t0–t2). (b) Mode 2–4 (t1–t4). (c) Mode 7 (t6–t7). (d) Mode 8 (t7–t8).

Mode 3 (t2–t3): This mode begins when diodeDs2 is turned ON. Current iLsis determined by following equation, and this mode ends when current iLs reaches 0 A

$$i_{Ls}(t) = -\frac{V_{Cc}}{L_s}(t-t_2) + i_{Ls}(t_2), t_2 < t < t_3 \quad (6)$$

It is noted that diodesDs1andDs2are turned OFF under ZCS condition.

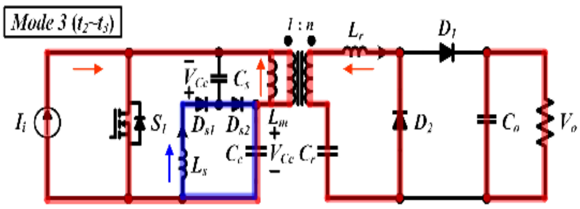

Mode4(t3–t4): The Lr–Cr resonance keeps on during this mode and ends when current iLr reaches 0 A. Note that diode D2is turned OFF under ZCS condition.

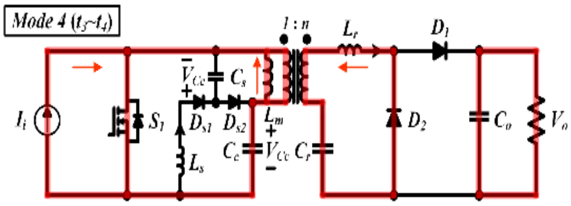

Mode5(t4–t5): During this mode, a constant current flows through S1 whose value is the sum of the input current Ii and the magnetizing current ILm.

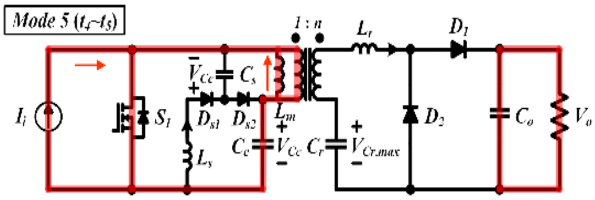

Mode6(t5–t6): The mode begins whenS1 is turned OFF. Then,Ii +ILm flows throughCs,Ds2, andCc. Voltage across snubber capacitor Cs which is determined by the following equation increases linearly with the slope of(Ii +ILm)/Cs, resulting in ZVS turn-off ofS1

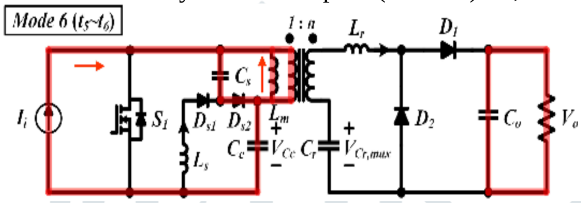

$$v_{Cs}(t) = \frac{I_i+I_{Lm}}{C_s}(t-t_5) - V_{cc}, \ t_5 < t < t_6 \qquad (7)$$

This mode ends when vCs becomes equal to (Vo− VCr,max)/n.

Mode 7 (t6–t7): This mode begins when diodeD1 is turned ON. Equivalent circuit of this mode is shown in Fig. 4(c).

Assuming that Cs << n2 Cr, vCr can be considered constant, and resonance frequencyωr3 can be determined by Cs and Lr. Therefore, the

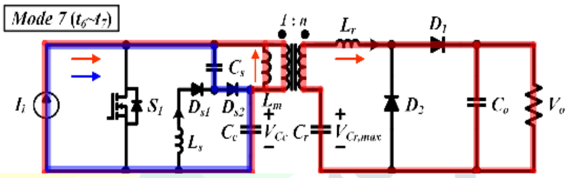

voltage and current of resonant components are determined, respectively, as follows:

$$i_{Lr}(t) = (I_i + I_{Lm})\left[1 - \cos\left(\omega_{r3}((t-t_6))\right), t_6 < t < t_7\right] \qquad (8)$$

whereωr3 =n/ √ LrCs. This mode ends when current iLrbecomes equal to(Ii +ILm)/n.

Mode 8 (t7–t8): This mode begins when diodeDs1 is turned ON. Equivalent circuit of this mode is shown in Fig. 5(d).

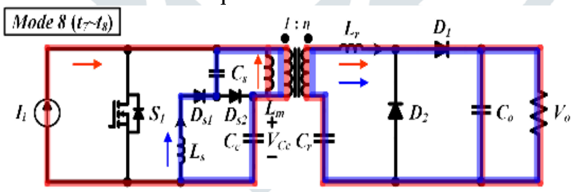

Assuming that Cs << n 2 Cr and Ls Lr/n 2 , the voltage and current of resonant components are determined using the superposition principle, respectively, as follows

$$i_{Ls}(t) = \left[V_{cc} + \frac{V_o}{n} - \left(V_{Cs,max} + \frac{V_{Cr,max}}{n}\right)\right] * \sqrt{\frac{C_s}{L_s}}\sin\left(\omega_{r2}(t-t_7)\right), t_7 < t < t_5 \qquad (9)$$

Mode 9 (t8–t9): SwitchS1is in the turn-off state, and the sum of the input current and magnetizing current is being transferred to the secondary. Current iD1 is equal to (Ii +ILm)/n.

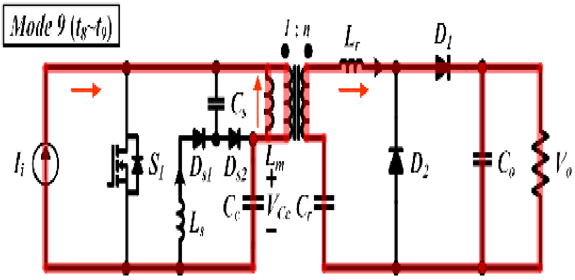

B. Voltage Gain Expression

To obtain voltage gain of the proposed converter, it is assumed that voltage across Cc is constant and magnetizing current is ignored during the switching period Ts.

1) Below-Resonance Operation (DTs >0.5Tr1): Since the average current of diodeD2 is identical to the average load current in the steady state, the following equation is obtained:

$$I_{D2,avg} = \frac{V_0}{R_0} = \frac{1}{T_S}\int_{t_1}^{t_4} i_{D2}(t)dt = \frac{1}{T_S}\int_{t_1}^{t_4} -i_{Lr}(t)dt \quad (10)$$

From (4) and (13), minimum voltage of the resonant capacitor VCr,min can be obtained by

$$V_{Cr,min} = nV_{CC} - \frac{V_O}{2C_r f_S R_0} \quad (11)$$

From (5) and (14), maximum voltage of the resonant capacitor VCr,max can be obtained by

$$V_{Cr,max} = nV_{CC} + \frac{V_O}{2C_r f_S R_0} \quad (12)$$

The time interval fromt7tot9in Fig. 3 can be obtained from (12) and (15) by

$$t_9 - t_7 = \frac{nV_0}{I_i f_S R_0} \quad (13)$$

The time interval fromt5tot6in Fig. 3 can be obtained from (7) by

$$t_6 - t_5 = \frac{C_S}{I_i}\left(\frac{V_O - V_{Cr,max}}{n}\right) + V_{CC} \quad (14)$$

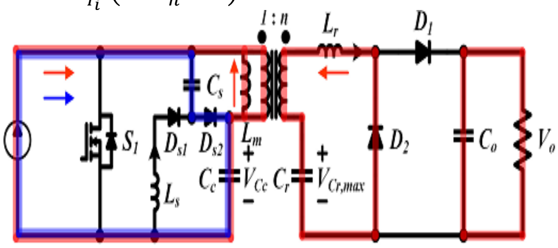

(a)

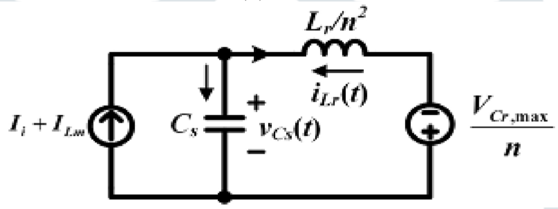

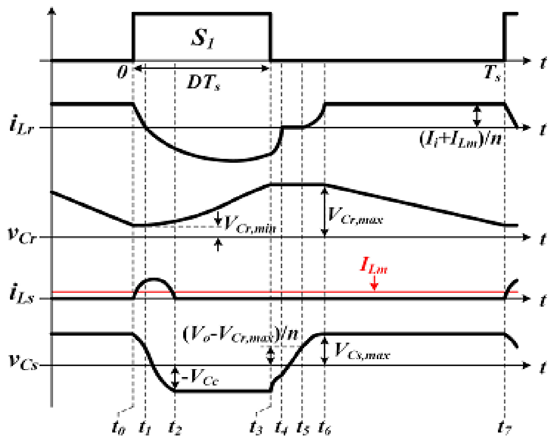

(b)

Fig. 5. Operation at time interval fromt3 tot4 in above resonance: (a) operation state. (b) Equivalent resonant circuit.

Fig. 6. Key waveforms of the proposed converter in the above-resonance operation.

2) Above-Resonance Operation (DTs <0.5Tr1):

Fig. 6 shows key waveforms of the proposed converter in the above resonance operation. The operating principles of the above resonance are the same as that of the below resonance except time interval fromt3 tot4. Assuming that Cs << n2 Cr, an equivalent circuit of time interval from t3 to t4 is shown in Fig. 5(b). The time interval fromt0 to t3 can be approximated as DTs. Since the average current of diodeD2is identical to the average load current, it can be approximated by

$$I_{D2,avg} = \frac{V_0}{R_0} \approx \frac{1}{T_S}\int_0^{DT_S} i_{D2}(t)dt \approx \frac{1}{T_S}\int_0^{DT_S} -i_{Lr}(t)dt \quad (15)$$

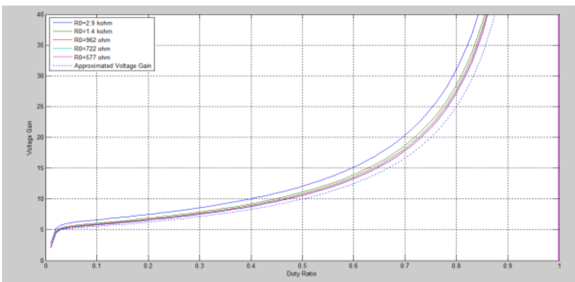

Fig. 7. Voltage gain of the proposed converter (Vi =28V,Lr =5μH, Cr = 560nF,Ls =5μH,Cs =16nF,n=5,fs = 100kHz).

C. Design Procedure

In this section, a design procedure of the proposed converter is presented with an example. However, if Cs is chosen to be small to reduce conduction loss of the snubber components, the voltage rating of the switch increases, as shown in (9), resulting in high conduction loss of the switch. Therefore, considering tradeoff between conduction losses of the switch and snubber components, ILs, avg is chosen to be around 3% of average input current, which is expressed as

$$I_{Ls,avg} = 0.03 I_{i,avg} = 0.27A \qquad (16)$$

1) Determine Values of n,Lr, and Cr: In order to simplify the design procedure, the voltage gain can be approximated as

$$\frac{V_0}{V_i} \approx \frac{n}{1-D} \qquad (17)$$

As mentioned earlier, the below-resonance operation is chosen for the proposed converter due to smaller switch turn-off current and diode di/dt. From Fig. 2, the minimum duty cycle for the below-resonance operation can be obtained by

$$D_{min} = \pi f_s \sqrt{L_r C_r} \qquad (18)$$

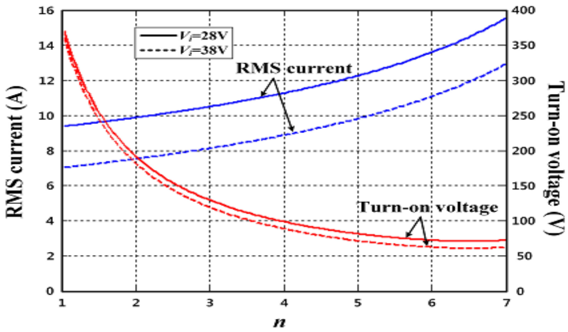

Fig. 8. RMS current and turn-on voltage of switchS1 with different values of n

2) Determine Value ofLs:

Snubber inductanceLsshould be designed to minimize reverse-recovery effects of snubber diodes Ds1andDs2. Therefore, the time interval fromt2tot3in Fig. 3 should be greater than3trr2, which is expressed as

$$t_3 - t_2 = 3t_{rr2} = \frac{vC_S(t_o)L_s \sin\left(cos^{-1}(-V_i/v_{CS}(t_o))\right)}{V_i}\sqrt{\frac{C_S}{L_S}} \qquad (19)$$

Where trr2 is reverse-recovery time of diodes Ds1andDs2. According to (34), snubber inductance Ls is calculated as 5μH.

3) Select Semiconductor Devices:

Semiconductor devices of the proposed converter are selected based on the previous design procedure and operating principles. It can be seen from Fig. 3 that output diodesD1andD2have a maximum voltage stress of Vo. Peak current of output diodeD2is0.5πIo/Dminfrom (10). Maximum voltage stress across the switchS1is determined by

$$V_{SI,max}(t) = \frac{I_i + I_{Lm}}{n}\sqrt{\frac{L_r}{C_s}} + \frac{V_o - V_{Cr,max}}{n} + V_{Cc} \qquad (20)$$

Current stress of switchS1is determined by (19). As shown in Figs. 3 and 4, maximum voltage stresses across snubber diodes Ds1 andDs2 are vCs(t0)+VCcandVCc, respectively. Peak currents of snubber diodesDs1 andDs2 arevCs(t0) Cs/Ls from (2) andIi , respectively. Selected devices and component ratings according to the previous design procedure are shown in Table I

TABLE I
COMPONENT RATINGS AND SELECTED DEVICES

Components		Rating	Selected devices
Switch S_1	V_{pk} I_{rms}	110 V 11.8 A	IRFP4568
Snubber diodes D_{s1}, D_{s2}	V_{pk} I_{avg}	94 V 0.27 A	UG8DT
Output diodes D_1, D_2	V_{pk} I_{avg}	380 V 0.65 A	VS-HFA04TB60
Filter inductor L_i	Inductance I_{rms}	100 μH 8.85 A	Ferrite core PQ32/30
Snubber inductor L_s	Inductance I_{rms}	5 μH 0.8 A	Ferrite core EF16
Snubber capacitor C_s	Capacitance V_{pk} I_{rms}	16 nF 82 V 1.4 A	BFC241941603
Clamp capacitor C_c	Capacitance V_{pk} I_{rms}	82 μF 38 V 7.6 A	FFB44D0826K
Transformer T_1	Leakage inductance Magnetizing inductance Turn ratio VA	5 μH 93 μH 1:5 273VA	Ferrite core PQ32/30
Resonant capacitor C_r	Capacitance V_{pk} I_{rms}	560 nF 196 V 1.6 A	ECW-FD2W564K4
Output capacitor C_o	Capacitance V_{pk} I_{rms}	1 μF 380 V 0.87 A	ECQ-E2W105KH

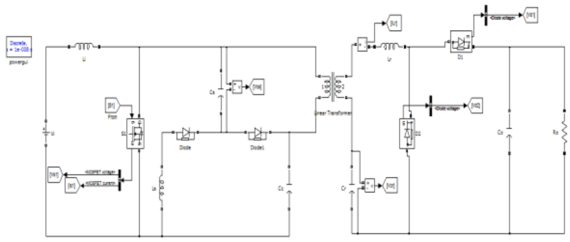

Fig.9 Block diagram of simulation

SIMULATION RESULTS

Figs. 10 and 11 show experimental waveforms at full-load and half-load conditions when input voltage is 28 V, respectively. Figs. 10(a) and 11(a) show that switch S1 is turned ON with ZCS at both full- and half-load conditions.

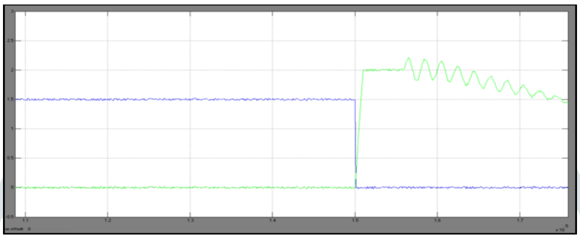

(a)

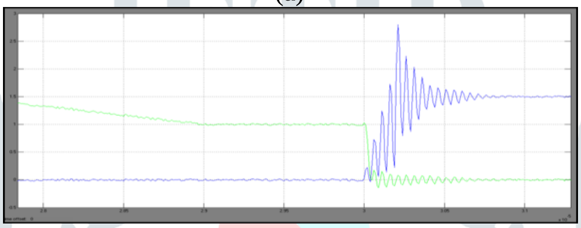

(b)

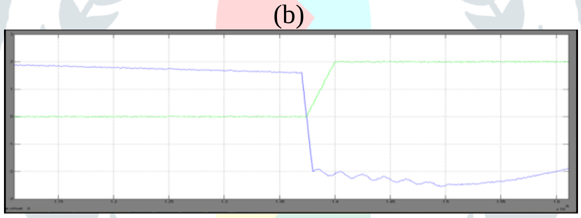

(c)

(d)

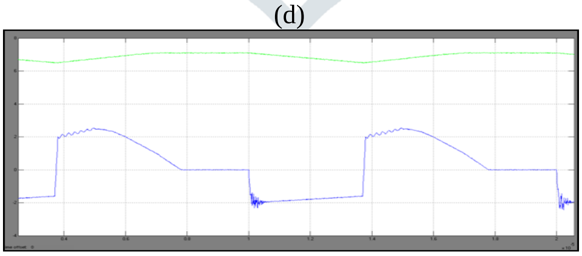

(e)

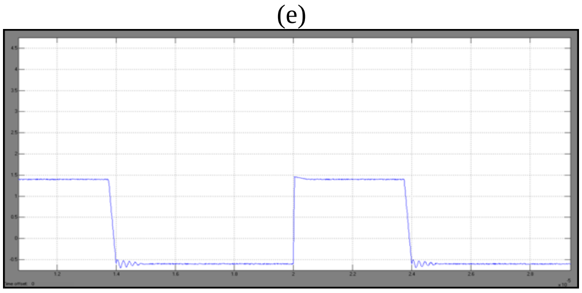

(f)

Fig. 10.Simulation waveforms atVi =28VandPo = 250W: (a) switch S1 at turn-on, (b) switchS1 at turn-off, (c) diodeD1 at turn-off, (d) diodeD2 at turn-off, (e) currentiLrand voltagevCr, and (f) voltagevCs.

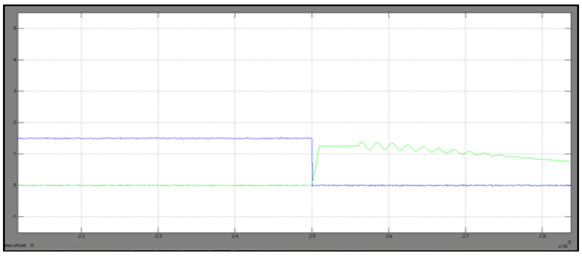
(a)

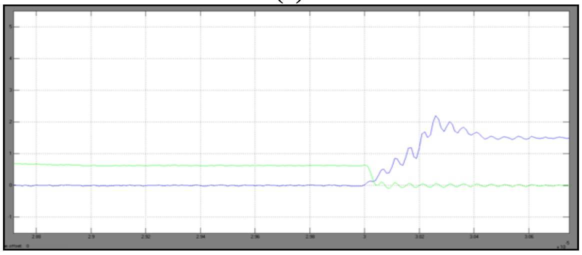
(b)

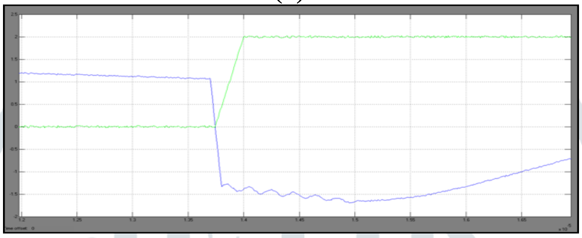
(c)

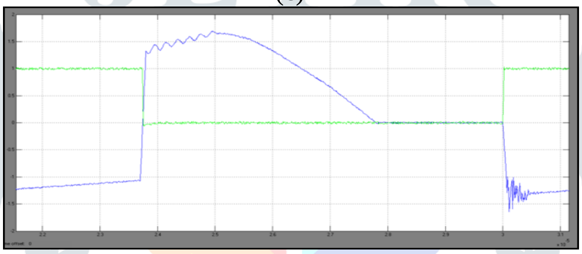
(d)

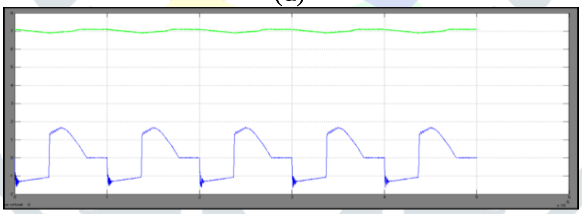
(e)

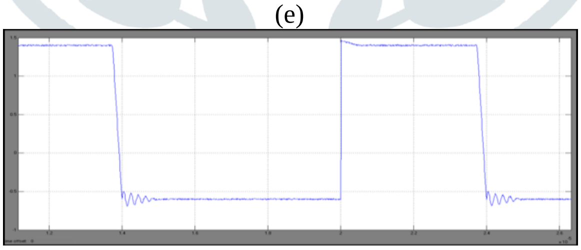
(f)

Fig. 11.Simulation waveforms atVi =28VandPo = 125W: (a) switch S1 at turn-on, (b) switchS1 at turn-off, (c) diodeD1 at turn-off, (d) diodeD2 at turn-off, (e) current iLr and voltage vCr, and (f) voltage vCs.

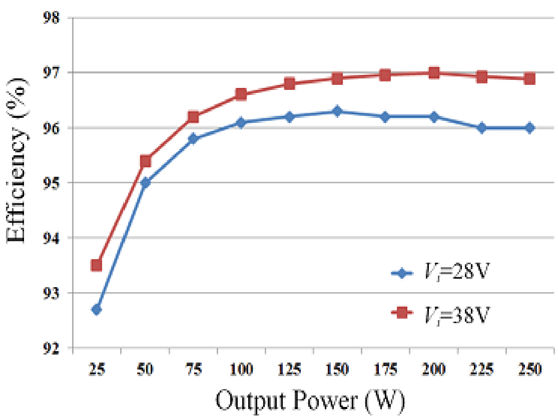

Fig. 12. Measured efficiency of the proposed converter.

IV. CONCLUSION

A soft-switched single switch isolated converter was proposed for step-up application such as MIC, portable fuel cell systems, and vehicle inverters is proposed in this paper. In this paper, a soft-switched single switch isolated converter is proposed for step-up application. The proposed converter has the following features: 1) ZCS turn-on and ZVS turn-off of switch regardless of voltage and load variation; 2) ZCS turn-off of all diodes leading to negligible voltage surge associated with the diode reverse recovery; 3) small input current ripple due to CCM operation; 4) reduced transformer volume due to low magnetizing current; and 5) low-rated lossless snubber, which makes it possible to achieve high efficiency and low cost for step-up application.

REFERENCES

[1] Q. Li and P. Wolfs, "A review of the single phase photovoltaic module integrated converter topologies with three different dc link configurations," IEEE Trans. Power Electron., vol. 23, no. 3, pp. 1320–1333, May 2008.

[2] N. D. Benavides and P. L. Chapman, "Mass-optimal design methodology for DC-DC converters in low-power portable fuel cell applications,"IEEE Trans. Power Electron., vol. 23, no. 3, pp. 1545–1555, May 2008.

[3] S. Y. Choe, J. W. Ahn, J. G. Lee, and S. H. Baek, "Dynamic simulator for a PEM fuel cell system with a PWM DC/DC converter,"IEEE Trans. Energy Convers., vol. 23, no. 2, pp. 669–680, Jun. 2008.

[4] H. Ma, L. Chen, and Z. Bai, "An active-clamping current-fed push-pull converter for vehicle inverter application and resonance analysis," inProc. IEEE Int. Symp. Ind. Electron., 2012, pp. 160–165.

[5] D. A. Ruiz-Caballero and I. Barbi, "A new flyback-current-fed push-pull DC-DC converter,"IEEE Trans. Power Electron., vol. 14, no. 6, pp. 1056– 1064, Nov. 1999.

[6] M. Nymand and M. A. E. Andersen, "High-efficiency isolated boost DCDC converter for high-power low-voltage fuel-cell applications,"IEEE Trans. Ind. Electron., vol. 57, no. 2, pp. 505–514, Feb. 2010.

[7] K. B. Park, G. W. Moon, and M. J. Youn, "Two-transformer current-fed converter with a simple auxiliary circuit for a wide duty range,"IEEE Trans. Power Electron., vol. 26, no. 7, pp. 1901–1912, Jul. 2011

[8] F. J. Nome and I. Barbi, "A ZVS clamping mode-current-fed push–pull DC–DC converter," inProc. IEEE Int. Symp. Ind. Electron., vol. 2, 1998, pp. 617–621.

[9] V. Yakushev, V. Meleshin, and S. Fraidlin, "Full-bridge isolated current fed converter with active clamp," in Proc. IEEE Appl. Power Electron. Conf. Expo., vol. 1, 1999, pp. 560–566.

[10] R. Watson and F. C. Lee, "A soft-switched, full-bridge boost converter employing an active clamp circuit," inProc. IEEE Conf. Power Electron. Spec. Conf. Rec., vol. 2, 1996, pp. 1948–1954.

[11] S. Han, H. Yoon, G. Moon, M. Youn, Y. Kim, and K. Lee, "A new active clamping zero-voltage switching PWM current-fed half-bridge converter," IEEE Trans. Power Electron., vol. 20, no. 6, pp. 1271–1279, Nov. 2005.

[12] J. Kwon and B. Kwon, "High step-up active-clamp converter with inputcurrent doubler and output-voltage doubler for fuel cell power systems," IEEE Trans. Power Electron., vol. 1, no. 1, pp. 108–115, Jan. 2009.

[13] H. Kim, C. Yoon, and S. Choi, "An improved current-fed ZVS isolated boost converter for fuel cell application,"IEEE Trans. Power Electron., vol. 25, no. 9, pp. 2357–2364, Sep. 2010.

[14] C. D. Davidson, "Zero voltage switching isolated boost converter topology," inProc. IEEE 33rd Int. Telecommun. Energy Conf., Oct. 2011, pp. 1–8.

[15] G. Spiazzi, P. Mattavelli, and A. Costabeber, "High step-up ratio flyback converter with active clamp and voltage multiplier,"IEEE Trans. Power Electron., vol. 26, no. 11, pp. 3205–3214, Nov. 2011.